JOURNAL OF BACTERIOLOGY, Oct. 1997, p. 6391–6399 Vol. 179, No. 20
0021-9193/97/$04.00+0

Three Genes of a Motility Operon and Their Role in Flagellar Rotary Speed Variation in *Rhizobium meliloti*

JOSEF PLATZER, WERNER STERR, MARTIN HAUSMANN, AND RÜDIGER SCHMITT*

Lehrstuhl für Genetik, Universität Regensburg, D-93040 Regensburg, Germany

Received 2 June 1997/Accepted 14 August 1997

The peritrichous flagella of *Rhizobium meliloti* rotate only clockwise and control directional changes of swimming cells by modulating flagellar rotary speed. Using Tn*5* insertions, we have identified and sequenced a motility (*mot*) operon containing three genes, *motB*, *motC*, and *motD*, that are translationally coupled. The *motB* gene (and an unlinked *motA*) has been assigned by similarity to the *Escherichia coli* and *Bacillus subtilis* homologs, whereas *motC* and *motD* are new and without known precedents in other bacteria. In-frame deletions introduced in *motB*, *motC*, or *motD* each result in paralysis. MotD function was fully restored by complementation with the wild-type *motD* gene. By contrast, deletions in *motB* or *motC* required the native combination of *motB* and *motC* in *trans* for restoring normal flagellar rotation, whereas complementation with *motB* or *motC* alone led to uncoordinated (jiggly) swimming. Similarly, a *motB-motC* gene fusion and a Tn*5* insertion intervening between *motB* and *motC* resulted in jiggly swimming as a consequence of large fluctuations in flagellar rotary speed. We conclude that MotC biosynthesis requires coordinate expression of *motB* and *motC* and balanced amounts of the two gene products. The MotC polypeptide contains an N-terminal signal sequence for export, and Western blots have confirmed its location in the periplasm of the *R. meliloti* cell. A working model suggests that interactions between MotB and MotC at the periplasmic surface of the motor control the energy flux or the energy coupling that drives flagellar rotation.

Motile bacteria swim by rotating helical flagellar filaments driven by a rotary motor in the cell membrane that is energized by the transmembrane gradient of protons (37, 41) or by sodium ions (20). The structure of bacterial flagella, their genetics, and the physiology of flagellar rotation have been extensively studied in members of the γ subgroup of proteobacteria, such as *Escherichia coli* and *Salmonella typhimurium* (for reviews, see references 22, 35, and 54).

In *E. coli*, the assembly, structure, and function of flagella require the products of some 50 genes. Among these, the motility proteins, MotA and MotB, and the switch proteins, FliM, FliN, and FliG, are necessary for flagellar rotation and for alternating between clockwise and counterclockwise rotation (30, 35). The membrane-bound proteins, MotA and MotB, are essential for torque generation (2–4, 63, 65). These proteins are known to function in transmembrane proton conduction, and MotB may also serve as an anchor that attaches the stator (the nonrotating portion of the motor) to the peptidoglycan layer (7, 9, 26, 61, 67). MotA-MotB complexes probably correspond to the 11 or 12 "studs" seen in electron micrographs as rings of intramembrane particles encircling the flagellar rod (24). Furthermore, averaged electron cryomicrographic images of the basal body have revealed a bell-shaped structure, named the C ring, that is attached to the cytoplasmic face of the basal body (13) and contains the switch proteins, FliM, FliN, and FliG, essential for flagellar rotation and direction control (21, 25, 36, 59).

Rhizobium meliloti, a member of the α subgroup of proteobacteria (45), exhibits distinctive differences from the enterobacterial paradigm (15, 16). An *R. meliloti* cell has typically 5 to 10 peritrichously inserted complex flagella, their filaments consisting of four related flagellin subunits (47, 56). The complex flagellar filaments form right-handed helices capable of limited polymorphic transitions but, as a result of helical ridges on their cylindrical surface, are unable to switch handedness (66). Accordingly, flagellar rotation in *R. meliloti* is unidirectionally clockwise, and swimming cells respond to tactic stimuli by modulating the flagellar rotary speed (60). Rotary speed is controlled by two response regulators, CheY1 and CheY2, and it has been postulated that their phosphorylation by CheA autokinase acts to slow the flagellar motor (60).

Both unidirectional rotation and speed variation are new features that prompted this study of the genetic basis of motility in *R. meliloti*. We report here the analysis of three closely linked motility genes, *motB*, *motC*, and *motD*, forming the *mot* operon. Whereas the unlinked *motA* gene (62) and *motB* are analogs of two familiar enterobacterial *mot* genes, *motC* and *motD* encode additional functions related to the new mode of flagellar rotation.

MATERIALS AND METHODS

Bacterial strains and plasmids. Derivatives of *E. coli* K-12 and *R. meliloti* MVII-1 (23) and plasmids used in this study are listed in Table 1.

Media and growth conditions. *E. coli* strains were grown in LB medium (34) at 37°C. *R. meliloti* strains were grown in TYC (0.5% tryptone, 0.3% yeast extract, 0.13% $CaCl_2 \cdot 6H_2O$ [pH 7.0]) or in RB minimal medium supplemented with vitamins and 0.2% mannitol as the sole carbon source (14) at 30°C. Agar plates were solidified with 1.5% Bacto Agar (Difco). Single colonies were transferred by toothpick onto swarm plates containing RB salts, 10^{-4} M mannitol, and 0.3% agar and incubated at 30°C for 2 days. Tn*5* mutagenesis was conducted as previously described (16). For optimum numbers of swimming cells, *R. meliloti* (10^8 cells/ml) was starved overnight in RB medium without mannitol, sedimented by centrifugation at room temperature, resuspended in an equal volume of RB medium with 0.2% mannitol, and grown in a rotary shaker (New Brunswick Scientific Co., New Brunswick, N.J.) at 30°C to 3×10^8 cells per ml (about 4 h).

Cloning of motility genes. Tn*5*-tagged chromosomal *Eco*RI fragments of mutant strains RU11/112 and RU11/113 were cloned into pIC20R and used to transform *E. coli* JM109 as described by Sambrook et al. (51). Transformants containing a Tn*5* insertion were selected on LB agar plates supplemented with ampicillin (100 μg per ml) and kanamycin (40 μg per ml). Adjacent fragments were obtained by partial *Eco*RI digestion of RU11/113 DNA. The resulting plasmids, pRU1213, pRU1212, pRU2064, and pRU2005 (Table 1), were used for sequence analysis.

* Corresponding author. Mailing address: Lehrstuhl für Genetik, Universität Regensburg, D-93040 Regensburg, Germany. Phone: 49 (941) 9433162. Fax: 49 (941) 9433163. E-mail: rudy.schmitt@biologie.uni-regensburg.de.

TABLE 1. Bacterial strains and plasmids used

Strain or plasmid	Markers[a] or derivation	Reference or source
E. coli		
JM109	*recA1 endA1 gyrA96 thi hsdR17 supE44 relA1* Δ(*lac proAB*)/F′ *traD36 proAB lacI*^{q}ZΔM15	68
S17-1	*recA endA thi hsdR* RP4-2-Tc::Mu::Tn*7* Tp^r Sm^r	58
BL21(DE3)	F$^-$ *ompT lon* (r_B^- m_B^-)	64
R. meliloti		
RU11/001	Sm^r; spontaneous streptomycin-resistant derivative of RU10/406 (wild type)	27
RU11/112	Sm^r Neo^r; Tn*5* insertion derivative of RU11/001, uncoordinated (jiggly) swimming	This study (Fig. 2)
RU11/113	Sm^r Neo^r; Tn*5* insertion derivative of RU11/001, paralyzed (Mot$^-$)	This study (Fig. 2)
RU11/211	Sm^r; deletion in *motC*, paralyzed (Mot$^-$)	This study (Fig. 2)
RU11/212	Sm^r; deletion in *motD*, paralyzed (Mot$^-$)	This study (Fig. 2)
RU11/213	Sm^r; fusion of *motB* and *motC* (jiggly)	This study (Fig. 3)
RU11/218	Sm^r, deletion in *motB*, paralyzed (Mot$^-$)	This study (Fig. 2)
RU11/215	Sm^r Gm^r Neo^r; RU11/211 (pRU2014)	This study
RU11/216	Sm^r Gm^r Neo^r; RU11/212 (pRU2015)	This study
RU11/219	Sm^r Gm^r Neo^r; RU11/218 (pRU2016)	This study
RU11/513	Sm^r; *motB* and *motC*, in-frame deletion, paralyzed (Mot$^-$)	This study (Fig. 2)
RU11/514	Sm^r Gm^r Km^r; RU11/513 (pRU1902)	This study
Plasmids		
pIC20H/R	Ap^r	38
pUCBM20	Ap^r	Boehringer Mannheim
pML122	Gm^r	29
pET19B	Ap^r	64
pK18*mobsac*B	Km^r	53
pRU1212	Ap^r Km^r; in vitro recombinant of pIC20R and 3.8-kbp *Eco*RI fragment of *R. meliloti* RU11/112 with Tn*5* inserted between *motB* and *motC*	This study
pRU1213	Ap^r Km^r; in vitro recombinant of pIC20R and 3.8-kbp *Eco*RI fragment of *R. meliloti* RU11/113 with Tn*5* inserted in *motC*	This study
pRU1902	Gm^r Km^r; in vitro recombinant of pML122 and 3.0-kbp fragment containing *motB* and *motC*	This study
pRU2005	Ap^r Km^r; in vitro recombinant of pIC20R and 7.7-kbp *Eco*RI fragment of *R. meliloti* RU11/113	This study
pRU2014	Gm^r Km^r; in vitro recombinant of pML122 and 1.3-kbp fragment containing *motC*	This study
pRU2015	Gm^r Km^r; in vitro recombinant of pML122 and 1.6-kbp *Sfu*I-*Bam*HI fragment containing *motD*	This study
pRU2016	Gm^r Km^r; in vitro recombinant of pML122 and 1.2-kbp PCR-generated fragment containing *motB*	This study

[a] Nomenclature according to Bachmann (1) and Novick et al. (44).

DNA methods. Chromosomal DNA from *R. meliloti* was extracted from lysozyme-treated cells and purified by dye-buoyant density centrifugation as previously described (48). For PCR, chromosomal DNA was extracted from single colonies of *R. meliloti* taken from an agar plate. Colonies were suspended in 100 μl of distilled water mixed with glass beads and one aliquot of phenol, agitated on a Vortex mixer for 1 min, incubated at 65°C for 5 min, and mixed, and debris was sedimented at 14,000 rpm for 5 min. The aqueous phase was extracted twice with one aliquot of chloroform; the DNA was ethanol precipitated and used for PCR. Plasmid DNA for sequence analysis was purified by the method of Li and Schweizer (32) optimized for GC-rich DNA templates, and PCR-amplified DNA was cloned by DISEC-TRISEC techniques (11). DNA was sequenced as described by Sanger et al. (52), using a Quick Denature Sequenase kit from Amersham Buchler (Braunschweig, Germany) and the supplier's protocol.

Expression of reMotC and antibody preparation. Recombinant MotC (reMotC) proteins, either complete (starting at Met1) or truncated (starting at Met36 [see Fig. 3]) were obtained by ligation to a 5′ leader sequence encoding a His tag positioned under the isopropylthiogalactopyranoside (IPTG)-inducible T7 promoter of pET19B and overexpressed in *E. coli* BL21(DE3) (50, 64). Low yields of complete reMotC and high yields (approximately 15 mg from ca. 10^{11} *E. coli* cells) of truncated reMotC (lacking the hydrophobic signal sequence) were obtained and purified by Ni-nitrilotriacetic acid affinity chromatography (Qiagen) to near homogeneity as monitored by sodium dodecyl sulfate-polyacrylamide gel electrophoresis. Polyclonal antibody against purified truncated reMotC was prepared from rabbits as described previously (40) or produced commercially (Eurogentec, Seraing, Belgium). The crude antiserum (0.5 ml) was purified by sequential depletion against 1-ml extracts of *E. coli* BL21(DE3) and the MotC-deficient *R. meliloti* RU11/513 (Table 1), each at 4°C for 60 min. Precipitating material was sedimented (16,000 × *g*, 30 min, 4°C), and the supernatant was run through a Sepharose-protein A column (Pharmacia, Freiburg, Germany). Antibody contained in the eluate was further purified by chromatography on reMotC bound to CNBr-activated Sepharose (Pharmacia). Aliquots of the purified antiserum were stored at −20°C and used at 1:200 dilution.

Cell fractionation. For membrane preparations, approximately 5×10^{10} motile *R. meliloti* cells were harvested by centrifugation (5,000 × *g*, 5 min), washed twice in 1 volume of 100 mM Tris-HCl (pH 8.0) at 4°C, and resuspended in 80 ml of 30 mM Tris-HCl (pH 8.0) containing 20% sucrose. After addition of 10 mM K_2-EDTA (pH 7.0) and 0.5 μg of lysozyme (final concentrations), protoplasts formed during a 30-min period of gentle stirring at room temperature. These were sedimented by centrifugation (16,000 × *g*, 10 min, 4°C) and resuspended in 0.5 ml of lysis buffer (0.1 M KP_i [pH 6.6], 20% sucrose, 20 mM $MgSO_4$), and 5 μg each of DNase and RNase were added. Protoplasts were lysed by dilution in 80 ml of KP_i (pH 6.6) and incubation at 37°C for 15 min under vigorous agitation; the mixture was adjusted to 10 mM K_2-EDTA (pH 7.0) and 15 mM $MgSO_4$ and incubated again for 15 min. Cell debris was collected by centrifugation (16,000 × *g*, 30 min), and the supernatant containing membranes was sedimented (45,000 × *g*, 12°C, 30 min). The pellet was resuspended in buffer (100 mM KP_i [pH 6.6], 10 mM EDTA), and the procedure was repeated four to six times to yield pure membranes. The periplasmic fraction was prepared by the polymyxin method (31, 39). About 5×10^{10} motile cells were harvested (4,000 × *g*, 10 min, 4°C), washed with 1 ml of buffer A (50 mM NaCl, 2 mM morpholinepropanesulfonic acid [MOPS] [pH 7.5]), sedimented again (5,000 × *g*, 10 min, 4°C), and resuspended in 600 μl of buffer B (10 mM MOPS, 5 mM EDTA, 5 mM Pefabloc [Merck, Darmstadt, Germany]) containing 2 mg of polymyxin B (Sigma, Munich, Germany) per ml. Polymyxin B permeabilizes outer membranes of gram-negative bacteria without affecting the cytoplasmic contents, thereby releasing the periplasm into the medium (31). After 60 min of incubation at 4°C, cells were sedimented (16,000 × *g*, 30 min, 4°C). Centrifugation of the supernatant (400,000 × *g*, 120 min, 4°C) yielded a small pellet that was carefully resuspended in 20 μl of H_2O and used for immunoblot analysis. The cytoplasmic fraction was prepared from polymyxin B-treated cells after harvesting (5,000 ×

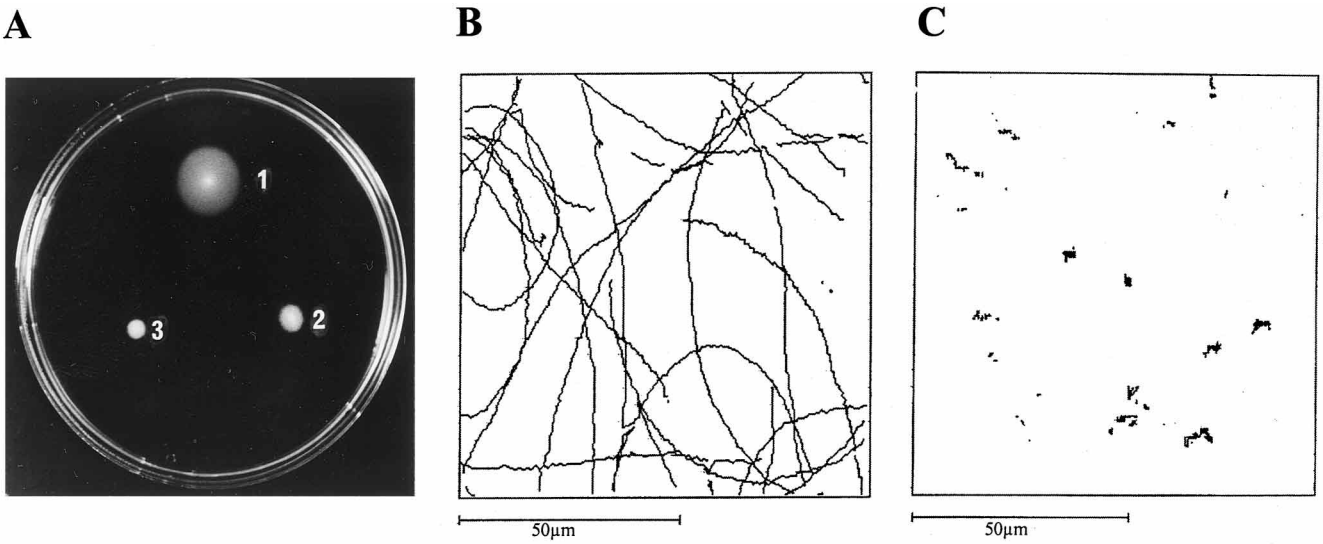

FIG. 1. (A) Swarm test of wild-type *R. meliloti* RU11/001 (swarm 1), the Tn*5*-induced jiggly mutant RU11/112 (swarm 2), and the Tn*5*-induced paralyzed mutant RU11/113 (swarm 3). Strains to be tested were transferred by toothpick onto swarm plates containing 10 mM mannitol and incubated at 30°C for 2 days. The diameter of a swarm ring reflects the motile proficiency of the respective strain. (B and C) Swimming paths of wild-type *R. meliloti* RU11/001 (B) and jiggly mutant RU11/112 (C). Swimming cells were monitored by computerized motion analysis.

g, 5 min) and resuspension in 1 volume of 50 mM Tris (pH 6.6)–10 mM EDTA by three passages through a French press at 10,000 lb/in^2. The resulting extract was freed of cell debris by centrifugation (45,000 × *g*, 30 min). Total cell extracts were obtained by the same procedure without polymyxin B treatment, starting from 5×10^{10} intact motile cells.

Alkaline phosphatase and β-galactosidase served as marker enzymes for the periplasmic and cytoplasmic fractions, respectively (33). Alkaline phosphatase activity was determined by the hydrolysis of *p*-nitrophenyl phosphate (Sigma) as described by Brickman and Beckwith (6), and β-galactosidase was assayed by hydrolysis of *o*-nitrophenyl-β-D-galactopyranoside (Sigma) as described by Miller (42).

Western blotting. Samples containing 30 to 50 μg of protein were separated on a 0.1% sodium dodecyl sulfate–12% polyacrylamide gel at 30 mA for 90 min, transferred to nitrocellulose, treated with 1% blocking reagent (Boehringer Mannheim) for 60 min, washed once with 0.5% blocking reagent, and then incubated overnight at room temperature with anti-reMotC antiserum (1:200 dilution). The nitrocellulose membrane was washed twice with TBS-T (20 mM Tris-HCl, 138 mM NaCl, 0.2% Tween 20) and 0.5% blocking reagent for 15 min each time. Bands were visualized by chemiluminescence using goat anti-rabbit antibody (1:2,000) complexed with peroxidase and an enhanced chemiluminescence detection kit (Boehringer Mannheim).

Deletion by allele substitution. Deletions were generated in vitro by using two PCR steps as described by Higuchi (19). PCR products containing the desired deletion were cloned into the mobilizable suicide vector pK18*mobsac*B (53) and used to transform *E. coli* S17-1. Filter crosses of *E. coli* and *R. meliloti* were performed as described by Simon et al. (58). Exconjugant *R. meliloti* cells were selected on TYC agar supplemented with neomycin (120 mg per ml) and streptomycin (600 mg per ml) for counterselection of *E. coli* at 30°C. Single colonies of *R. meliloti* (containing cointegrated plasmid DNA) were grown overnight in TYC to allow resolution and homologous recombination to occur. Selection on RB agar supplemented with 20% sucrose (55) at 30°C yielded colonies that had lost the *sacB*-containing vector. These were screened for neomycin sensitivity and for swarming proficiency. All colonies exhibiting unusual swarming behavior (approximately 1 in 200) were monitored by PCR and Southern hybridization to determine whether the mutant phenotype resulted from a directed deletion in the target gene. Complementation with pML122-based recombinant genes (Table 1) was performed as described by Labes et al. (29).

Motion analysis. Motility and swimming patterns of *R. meliloti* were observed by phase-contrast microscopy (Zeiss Standard 14 microscope; Zeiss, Oberkochen, Germany). Free-swimming tracks were analyzed by computerized motion analysis using a Hobson BacTracker (Hobson Tracking Systems, Ltd., Sheffield, England) as previously described (60).

Nucleotide sequence accession number. The sequence shown in Fig. 3 has been deposited in GenBank under accession no. L49337.

RESULTS

Transposon mutagenesis. Insertion mutagenesis and tagging with transposon Tn*5* were used to identify genes encoding components of the *R. meliloti* flagellar motor. Of 8,000 colonies screened on swarm plates, two motility mutants, RU11/112 and RU11/113, were isolated. These were examined electron microscopically and were found to possess intact flagella. Strain RU11/113 was nonmotile on swarm plates (Fig. 1A) and on inspection by phase-contrast microscopy. By contrast, strain RU11/112 formed small swarm rings (Fig. 1A), and motion analysis revealed cells that rotated (jiggled) around their axis or swam in tiny spirals (Fig. 1C). If tethered by a single flagellum, single unidirectionally rotating cells exhibited extreme fluctuations of rotary speed (data not shown).

Physical map. Southern hybridization of genomic DNA from mutants RU11/112 and RU11/113 detected single transposon insertions. Chromosomal fragments obtained after *Eco*RI digestion of RU11/112 and RU11/113 DNA were cloned into plasmid pIC20R and then used to transform *E. coli* JM109. Tn*5*-containing fragments identifiable by their resistance to kanamycin were physically mapped. The paralyzed mutant RU11/113 and the jiggly mutant RU11/112 contained Tn*5* inserted into identical 3.8-kbp *Eco*RI fragments. Sequence analysis (below) confirmed that the two Mot phenotypes represent two alleles of a new motility gene, named *motC*. A chromosomal walk from the transposition sites led to the identification of a 7.7-kbp genomic region including three closely linked open reading frames (Fig. 2). These were assigned as *mot* on the basis of in-frame deletions introduced in *motB* (strain RU11/218), *motC* (strain RU11/211), and *motD* (strain RU11/212) each resulting in paralyzed cells with intact flagella. Translational coupling of the three genes (46), the interdependence of the encoded functions (shown below), and common upstream promoter and downstream terminator sequences (Fig. 3) all suggest that *motB-motC-motD* form an operon. The physical map (Fig. 2) depicts gene sizes and their polarity, Tn*5* insertions resulting in two different MotC phenotypes, and the

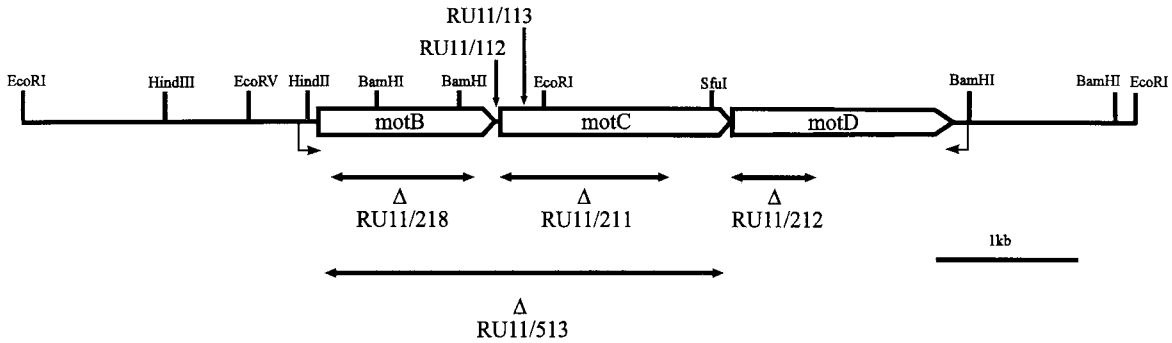

FIG. 2. Physical and genetic map of a composite 7.7-kbp *Eco*RI fragment containing three genes, *motB*, *motC*, and *motD*, of the *R. meliloti mot* operon. Pointed open boxes mark the polarity and extent of genes. Sites of Tn*5* insertions inducing the jiggly (RU11/112) and paralyzed (RU11/113) phenotypes are indicated by vertical arrows. The extents of deletions introduced in *motB* (RU11/218), *motC* (RU11/211), *motD* (RU11/212), and *motB-motC* (pRU11/513), respectively, are indicated by two-pointed arrows. Hooked arrows define the 4.2-kbp sequenced portion shown in Fig. 3.

extent of in-frame deletions introduced to define gene functions.

Nucleotide sequence and gene assignments. The 4,196-bp nucleotide sequence that contains the *mot* operon and flanking DNA is presented together with deduced polypeptide sequences in Fig. 3. Gene assignments were made by using the similarity to the *E. coli* homolog (*motB*) and by phenotypes of deletion mutants delineated in Fig. 2. The sequence of a *motA* homolog encoding a protein of 63% similarity to the *E. coli* MotA and mapping 21 kbp upstream on the *R. meliloti* chromosome has been deposited in a data library (GenBank accession no. U87913) and will be described elsewhere. Close linkage of the other three *mot* genes—*motB* extends from nucleotides 202 to 1387 (394 codons), *motC* extends from nucleotides 1390 to 2694 (434 codons), and *motD* extends from nucleotides 2691 to 4118 (475 codons)—indicates operon structure, and the juxtaposition of genes with a putative ribosome-binding site overlapping the upstream open reading frame (Fig. 3) suggests translational coupling (46). A σ^{28}-like promoter motif (18) upstream of *motB* and a short terminator palindrome followed by thymidine residues downstream of *motD* are marked as candidate transcription signals for a polycistronic mRNA (Fig. 3). Yet, Northern analysis and the unambiguous assignment of transcription initiation by primer extension were obviated by low-level *mot* mRNA.

Functional assignments. (i) MotB. The derived 394-residue MotB polypeptide of *R. meliloti* exhibits 34% identity and 55% similarity to the *E. coli* MotB (61) but is distinctly longer than those of *E. coli* (308 amino acid residues [61]) and *Bacillus subtilis* (261 residues [43]), due to a large insertion between residues Gln71 and Ser204 (Fig. 4). On the other hand, regions essential for function are well conserved: the hydrophobic region between residues Lys33 and Ala54 closely resembles the proposed membrane-spanning α helix of *E. coli* MotB (7, 61), with a conserved Asp37 thought to participate in transmembrane proton conduction together with charged residues of four α-helical domains of MotA (4, 8). Furthermore, a peptidoglycan-binding motif, identified in *E. coli* and *B. subtilis* MotB proteins and in OmpA-related outer membrane proteins (9, 26), is conserved in the *R. meliloti* MotB protein (Asn335 to Leu350 and aligned consensus motif in Fig. 4). It has been proposed that the association of this domain with the peptidoglycan layer serves to anchor the MotA-MotB complex to the cell wall (7). Moreover, residues that affect the function of MotB in *E. coli* (5) (highlighted in Fig. 4) are highly conserved.

Complementation of the paralyzed *motB* deletant RU11/218 with an intact *motB* overexpressed under neomycin promoter control (strain RU11/219) restored less than 30% of swarming proficiency (Fig. 5B). Motion analysis of free-swimming RU11/219 cells revealed considerable reductions in absolute (−23%) and relative (−40%) speed and hence a low smooth-swimming rate (Table 2). This was similarly observed when the paralyzed *motC* deletant RU11/211 was complemented with an intact *motC* gene (RU11/215): swarming (Fig. 5C) as well as absolute (−18%) and relative (−52%) free-swimming speed was greatly reduced, and so was the smooth-swimming rate (Table 2). Likewise, overexpression of a plasmid-borne *motB* or *motC* gene in wild-type *R. meliloti* RU11/001 had an adverse, semidominant effect on motility, very similar to that seen in the Δ*motB* mutant complemented with an intact *motB* gene (Δ*motB*/*motB*) and Δ*motC*/*motC* complementation experiments (Fig. 5 and Table 2). The values range in between those of wild-type RU11/001 and the jiggly mutant RU11/112, because the merodiploids always formed mixed populations of normal and jiggly swimmers.

These data clearly indicate that a subtly balanced synthesis of the *motB* and *motC* gene products is absolutely required for coordinated flagellar rotation. Consistent with this notion is the motile behavior of a merodiploid (RU11/514) that carries a chromosomal *motB-motC* deletion and the native *motB-motC* configuration on the complementing plasmid, pRU1902. This strain with an increased but balanced *motB-motC* gene expression exhibited near-normal swarming (Fig. 5A) and free-swimming behavior (Table 2).

(ii) MotC. The derived MotC polypeptide (Fig. 3) has no known precedents in other bacteria. The protein possesses a

FIG. 3. Nucleotide sequence of a 4,196-bp *R. meliloti* genomic region (Fig. 2) containing the *mot* operon and deduced amino acid sequences. Numbers to the left run sequentially and refer to nucleotides (upper lines) and amino acid residues (lower lines). The 9-bp target sites of two Tn*5* insertions are doubly underlined and marked by mutant strain numbers. Presumptive promoter boxes (−10, −35), transcription termination (←·→), ribosome-binding sites (SD), translation starts (gene assignments), and stops (*) are indicated. Dotted underlining marks the extent of deletions introduced to yield RU11/218 (Δ*motB*), RU11/211 (Δ*motC*), and RU11/212 (Δ*motD*); the large deletion RU11/513 (Δ[*motB-motC*]) is delimited by vertical lines. Six nucleotides (TGAGAA) deleted to fuse *motB* and *motC* (RU11/213) are boxed. Cloned fragments used for complementation analysis are delimited by hooked arrows with plasmid assignments (Table 1; Fig. 2). The vertical arrow marks the putative signal peptidase cleavage site in MotC.

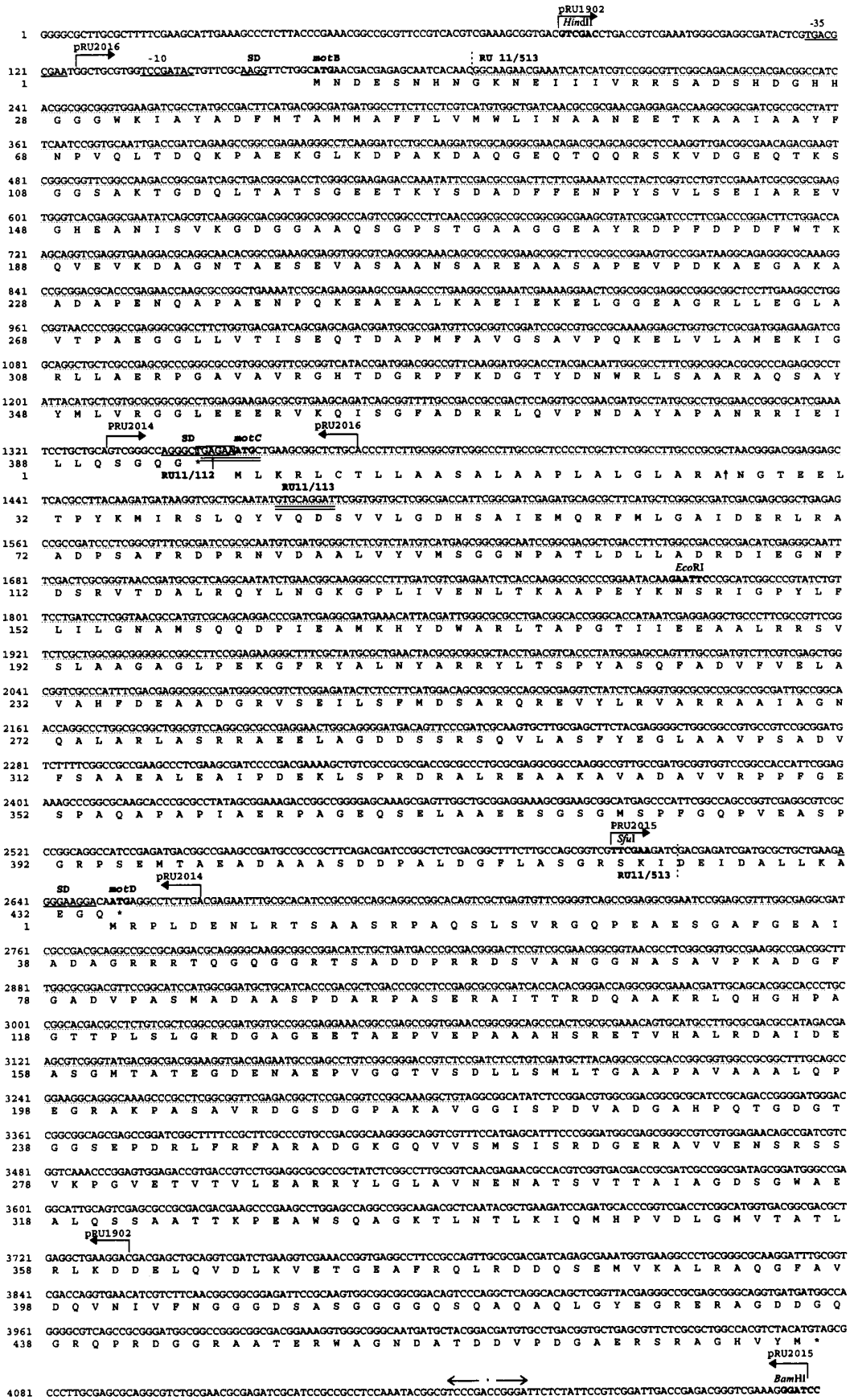
pRU1902
HindII
-35
pRU2016
-10
SD
motB
RU 11/513
PRU2014
SD
motC
pRU2016
RU11/112
RU11/113
EcoRI
PRU2015
SfuI
RU11/513
pRU2014
SD
motD
pRU1902
pRU2015
BamHI

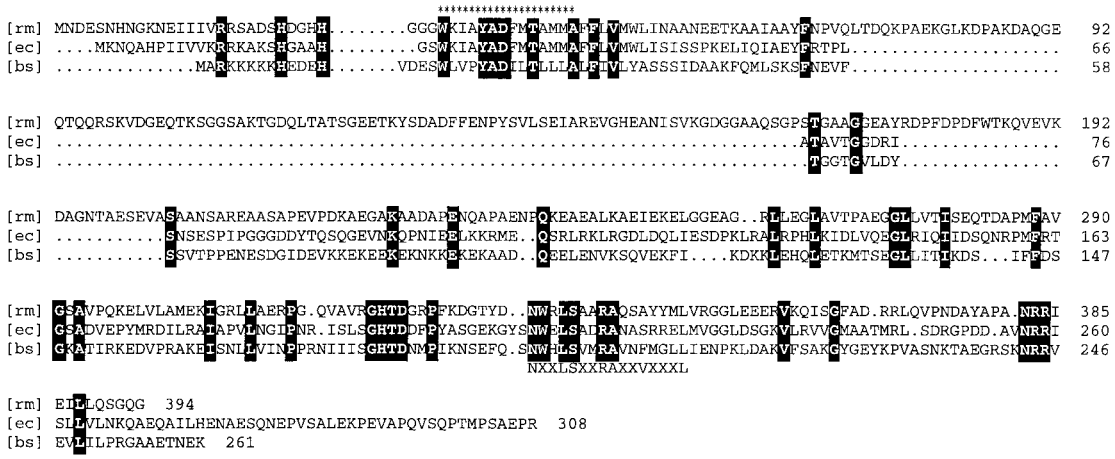

FIG. 4. (A) Aligned polypeptide sequences of *motB*-encoded proteins from *R. meliloti* ([rm]), *E. coli* ([ec]) (64), and *B. subtilis* ([bs]) (43). An α-helical domain (*) putatively spanning the membrane and containing an aspartate residue (↓) believed to participate in proton transfer is marked; conserved residues are highlighted by shading. A deduced peptidoglycan-binding domain is indicated by alignment with the consensus (X = any residue) (9, 26). Alignments were optimized by using PILEUP of the GCG program package (10).

typical signal sequence for secretion into the periplasm (49) with a short, positively charged N-terminal sequence (MLKR) followed by 16 mostly hydrophobic residues (LCTLLAASA LAAPLAL) and a signal peptidase I site (GLARA) with the consensus GX(X)AXA. A hydropathy plot of MotC (28) revealed no additional membrane-spanning domains, suggesting that the mature MotC protein is located in the periplasm.

This assertion was proven correct by Western blot analysis of crude cell extracts and cell fractions prepared from wild-type and mutant *R. meliloti* (Fig. 6). A polyclonal antiserum raised against recombinant MotC protein revealed a 53-kDa band, present in crude extracts and the periplasmic fraction (Fig. 6, lanes 1 and 4) but not in the cytoplasmic or membrane fractions (lanes 2 and 3) of wild-type RU11/001. The 53-kDa band was absent from a *motC* deletant (RU11/211 [lane 5]) but present in the periplasmic fraction if this strain carried a complementing *motC* gene (RU11/215 [lane 8]), thus proving the validity of this analysis. β-Galactosidase and alkaline phosphatase served as marker enzymes of the cytoplasmic and periplasmic fractions, respectively. The presence or absence of these enzymes in the cell fractions tested clearly demonstrated that these were properly assigned to the respective bacterial cellular compartments (data not shown).

Two Tn*5* insertions differentially affect *motC*. One insertion, separating the *motC* codons 45 and 46 (RU11/113 [Fig. 3]), resulted in paralysis, whereas the other (RU11/112 [Fig. 3]), 5

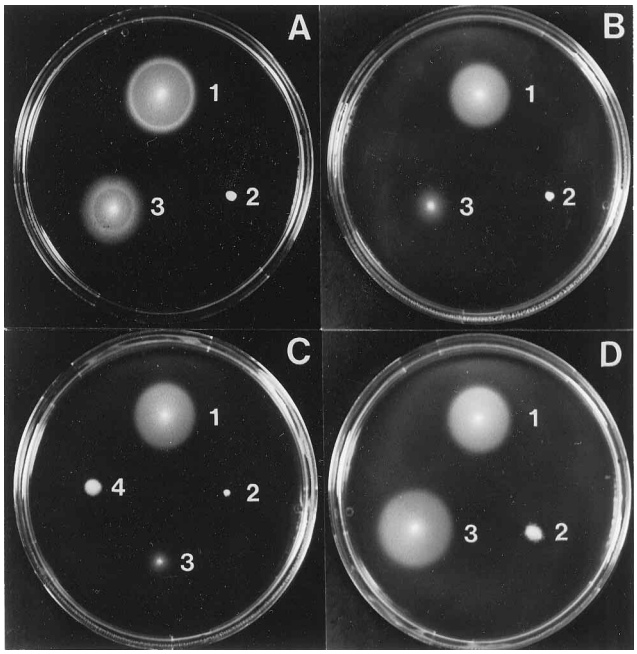

FIG. 5. Effects of deletions and *trans* complementation of *motB-motC* together and of *motB*, *motC*, and *motD* alone on swarming. See Table 1 for descriptions of the strains tested. (A) 1, RU11/001 (wild type); 2, RU11/513 (Δ[*motB motC*]); 3, RU11/514 (Δ[*motB motC*]/*motB-motC*). (B) 1, RU11/001; 2, RU11/218 (Δ*motB*); 3, RU11/219 (Δ*motB*/*motB*). (C) 1, RU11/001; 2, RU11/211 (Δ*motC*); 3, RU11/215 (Δ*motC*/*motC*); 4, RU11/213 (*motB-motC* fusion). (D) 1, RU11/001; 2, RU11/212 (Δ*motD*); 3, RU11/216 (Δ*motD*/*motD*). Experimental conditions were as for Fig. 1.

TABLE 2. Absolute and relative free-swimming speeds of wild-type and mutant *R. meliloti*[a]

Strain	V_{inst} (μm s^{-1})[b]	V_{sl} (μm s^{-1})[c]	V_{sl}/V_{inst}[d]
RU11/001 (wild type)	32.8 ± 0.4	25.8 ± 0.5	0.79
RU11/112 (Tn*5*::*motC*)	20.5 ± 0.6	10.9 ± 1.1	0.53
RU11/219 (Δ*motB*/*motB*)[e]	25.4 ± 1.2	15.3 ± 0.6	0.60
RU11/215 (Δ*motC*/*motC*)[e]	26.8 ± 1.4	12.3 ± 2.3	0.45
RU11/514 (Δ[*motB motC*]/*motB motC*)	31.6 ± 0.7	23.0 ± 1.0	0.73
RU11/216 (Δ*motD*/*motD*)	35.9 ± 0.9	26.0 ± 1.1	0.73

[a] Mean values of 100 to 300 individual cell tracks were determined from each sample by computerized motion analysis and were averaged from at least five independent cell populations.

[b] V_{inst}, instantaneous velocity; defines the velocity measured in every track point and averaged for the track (absolute speed).

[c] V_{sl}, straight-line velocity; defines the linear distance traveled per second between endpoints of a given track (relative speed).

[d] Smooth-swimming rate; represents the proportion of smooth swimming under a given condition.

[e] About 5% normal-swimming cells.

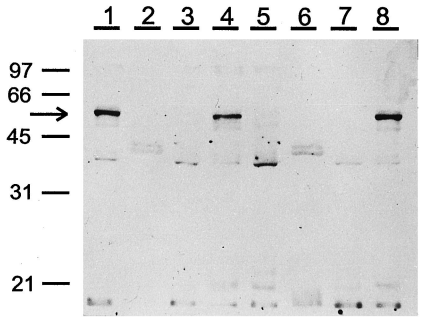

FIG. 6. Western blot analysis of crude extracts and of cell fractions from wild-type and mutant *R. meliloti*, using polyclonal anti-MotC antiserum raised against reMotC protein. Cell fractionation and visualization of bands by chemiluminescence are described in Materials and Methods. Arrow marks the MotC band with an apparent molecular weight of 53,000. Lanes 1 to 4, fractions from RU11/001 (wild type) (cell extract, membranes, cytoplasm, and periplasm, respectively); lane 5, RU11/211 (Δ*motC*), cell extract; lanes 6 to 8, fractions from RU11/215 (Δ*motC*/*motC*) (membranes, cytoplasm, and periplasm, respectively). Positions of molecular mass standards are indicated to the left in kilodaltons.

bp upstream of the *motC* translation start, resulted in jiggly swimming (Fig. 1). This insertion affects neither the TAG stop of *motB* nor the ATG start of *motC*, owing to a 9-bp sequence duplication generated by Tn*5*, but interrupts continuous transcription and the translation coupling of *motB* and *motC*. Conceivably, the Tn*5* insertion generates a weak promoter upstream of *motC* that leads to low-level transcription and reduced synthesis of MotC relative to MotB.

Furthermore, a *motB-motC* gene fusion generated by deletion of 6 bp—the *motB* stop codon plus 3 bp between *motB* and *motC* (Fig. 3)—resulted in a nonswarming mutant phenotype (RU11/213 [Fig. 5C]). When cells were grown in Bromfield medium, about 5% uncoordinated, jiggly-swimming cells were observed, whereas the majority of cells were paralyzed. Suppressor mutants that regained between 50 and 100% of wild-type swarming proficiency were isolated from swarm plates after 10 to 12 days of incubation at 30°C. PCR-based sequence analyses revealed intragenic suppression in *motB*, either by C-T transition at position 2178 or by deletion of a G at position 2176 or 2182 (Table 3). As a result, each suppressor mutant had a new *motB* stop codon and produced MotB variants with two amino acids deleted or added at the C terminus. The former regained 100% and the latter regained 50 to 60% of their swarming proficiency. These results suggest that the integrity of *motB* and *motC* genes is a prerequisite for normal motor function.

(iii) MotD. The third open reading frame, *motD*, encodes a 475-residue polypeptide. Database searches did not reveal any similarity with known proteins. The derived polypeptide contains no obvious membrane-spanning domains, nor has a signal peptide been detected. Therefore, MotD is likely to be a cytoplasmic protein, with an essential function in motility. A deletion of the 5′ half of *motD* (RU11/212 [Fig. 2]) rendered the cells paralyzed and nonswarming (Fig. 5D), though electron microscopy revealed normal flagellation. In contrast to results for *motB* and *motC*, complementation with an overexpressed native *motD* gene on plasmid pRU2015 (strain RU11/213 [Table 1]) even overcompensated for the swarming deficiency of the deletion mutant RU11/212 (Fig. 5D), and free-swimming speed was increased by 10% (Table 2). The results suggest that an enhanced dose of MotD positively affects flagellar rotary speed.

DISCUSSION

We have previously shown that *R. meliloti* responds to tactic stimuli by rotary speed control of its flagella (15, 60). The finding of two new *mot* genes, *motC* and *motD*, offers interesting possibilities for this new mode of flagellar rotation. By analysis of the encoded Mot proteins and various mutant phenotypes, it may be possible to assign functions to these motility proteins in a working model whose predictions can be tested.

Like in *E. coli*, the conserved MotA (62) and MotB (Fig. 4) proteins of *R. meliloti* are considered essential for energizing the flagellar motor. Four predicted membrane-spanning α helices of MotA and a single α helix of MotB are thought to form a proton-conducting channel (3–5). Based on topological data and sequence comparisons, MotB has been proposed as linker connecting the MotA-MotB stator complex to the cell wall (7, 9, 26). An analysis of unusual speed fluctuations in slow-swimming mutants of *E. coli* (mapped to the large periplasmic domain of MotB) indicated that in these mutants, the number of force-generating units was reduced (5). This observation is interesting in view of a possible mechanism for flagellar rotary speed variation that inherently directs the swimming pattern of *R. meliloti* cells (60).

The *motB* and *motC* genes of *R. meliloti* are closely linked in a way that implies coordinate expression and stoichiometric relationships between the gene products, MotB and MotC. This view is supported by the properties of mutants that alter the balance of transcription (strain RU11/112) or translation (strain RU11/213) and that either under- or overexpress MotC protein relative to MotB (strains RU11/215 and RU11/219 [Table 1]). Their jiggly swimming patterns reflect uncoordinated rotation of different flagella on a given cell, as evidenced by extreme fluctuations of rotary speed observed in tethered mutant cells (data not shown). Therefore, the correct stoichiometry and positioning of MotC relative to MotB, which is faulty in the abnormal swimmers, may be the key to controlling the rotary speed of a flagellum. The need for balanced biosynthesis of MotB and MotC may be explained by the sequence of events that requires the correct placing of MotB first to scavenge and position MotC correctly at the periplasmic surface of the flagellar motor (see below).

TABLE 3. Nucleotide changes, corresponding amino acid changes, and the effect on swarming in suppressor mutants of RU11/213 (*motB-motC* fusion)

motB allele(s)	Nucleotide change	Amino acid change	Swarming proficiency[a] (% of wild type)
213	ΔT2184–A2189	Fusion MotB-MotC	5
500, 505, 506	C2178→T	Gln393→stop	100
504	ΔG2176	Gly392 Gln393 Gly394→Ala Arg Ala Cys stop	50
508	ΔG2182	Gly394→Ala Cys stop	40

[a] Defined as the ratio of diameter of mutant swarm ring to diameter of wild-type swarm ring × 100 on a Bromfield swarm plate.

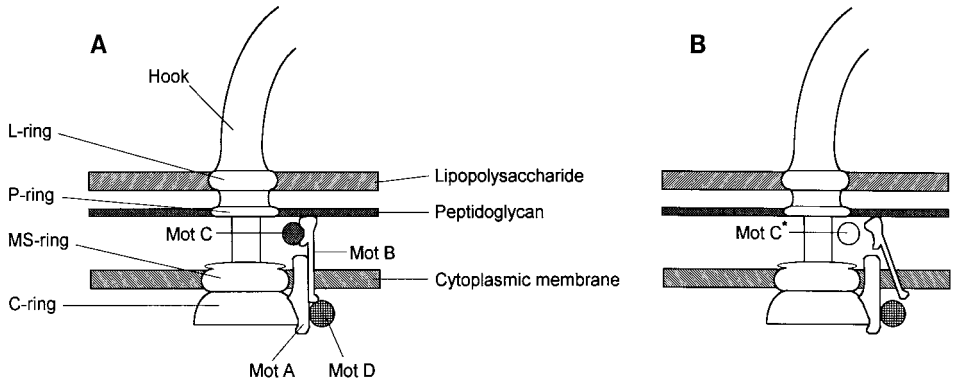

FIG. 7. Working model of the *R. meliloti* flagellar motor. The cartoon illustrates what is known about the basal body structure and its relation to layers of the cell envelope of gram-negative bacteria (13, 35). (A) The suggested interaction of MotC with the periplasmatic domain of MotB implicated in proton flux and the presumptive location of MotD at the cytoplasmic surface of the motor are depicted. We assume this to be the active configuration with a functional force-generating MotA-MotB complex. (B) Possible effect of a mutation or deletion in *motC* leading to a defective MotC* protein. The failure to bind to MotB is thought to result in loss of energy flux, as schematically indicated by distortion of the MotA-MotB complex.

The N-terminal amino acid sequence of the derived MotC polypeptide has features of a signal sequence (49) suggesting that MotC is secreted to the periplasm. This notion was proven correct by Western analysis of cell fractions that located MotC in the periplasm of the *R. meliloti* cell (Fig. 6). The antiserum-complexed MotC band was detectable in neither the cytoplasmic nor membrane fraction of wild-type *R. meliloti*, and it was completely lacking in the *motC* deletion strain RU11/211. The likely partner of a periplasmic MotC protein that exerts control over motor speed would be MotB protein with its large periplasmic domain (7). In fact, preliminary data obtained with cloned portions of *motB* and *motC* in the yeast two-hybrid system (12) indicate protein-protein interactions between MotC and the periplasmic portion of MotB (17).

These findings together with the properties of certain slow-swimming *E. coli motB* mutants (5, 65) are consistent with a working model that accounts for flagellar rotary speed control exerted by MotB-MotC interactions (Fig. 7). The model is based on the assumptions (i) that in *R. meliloti*, fluctuations of rotary speed are a function of the fraction of working MotA-MotB complexes (force-generating units or torque generators) acting on a given motor (24) and (ii) that interactions between MotB and MotC control the activity of individual force-generating units. MotB alone leaves a torque generator nonfunctional, but it becomes functional when MotB and MotC are complexed. A missing or defective MotC molecule thus arrests proton conduction or energy coupling of a force-generating MotA-MotB complex, a deficit that reduces the rotary speed of that motor. This model is consistent with the observed abnormal (jiggly) swimming pattern of mutants with an upset balance of MotB and MotC proteins (strains RU11/112, RU11/213, and RU11/215 [Fig. 5 and Table 2]), whose swimming behavior results from rotary speed fluctuations that prevent flagellar synchrony in a single cell.

MotD, the other new motility protein, has features of a cytoplasmic protein thought to be associated with the inner surface of the motor (Fig. 7). Complementation studies suggest that overexpression of *motD* even improves normal swarming or free-swimming motility (Fig. 5D and Table 2). MotD may be a cytoplasmic relay involved in transmitting signals from the response regulators, CheY1 and CheY2 (57), to the speed-controlling elements. If our current experiments (17) confirm the alleged role of MotB-MotC interactions in motor speed control, an elucidation of the signal pathway from cytoplasm to periplasm will be the topic of future studies.

ACKNOWLEDGMENTS

This work was supported by the Deutsche Forschungsgemeinschaft (Schm68/24-2) and by a DAAD travel grant (ARC).

We thank Judy Armitage for helpful discussion, Simon Silver for critical review of the manuscript, and Klaus Stark for artwork.

REFERENCES

1. **Bachmann, B. J.** 1990. Linkage map of *Escherichia coli* K-12, edition 8. Microbiol. Rev. **54:**130–197.
2. **Blair, D. F., and H. C. Berg.** 1988. Restoration of torque in defective flagellar motors. Science **242:**1678–1681.
3. **Blair, D. F., and H. C. Berg.** 1990. The MotA protein of *E. coli* is a proton-conducting component of the flagellar motor. Cell **60:**439–449.
4. **Blair, D. F., and H. C. Berg.** 1991. Mutations in the MotA protein of *Escherichia coli* reveal domains critical for proton conduction. J. Mol. Biol. **221:**1433–1442.
5. **Blair, D. F., D. Y. Kim, and H. C. Berg.** 1991. Mutant MotB proteins in *Escherichia coli*. J. Bacteriol. **173:**4049–4055.
6. **Brickman, E., and J. Beckwith.** 1975. Analysis of the regulation of *E. coli* alkaline phosphatase synthesis using deletions and 80 transducing phages. J. Mol. Biol. **96:**307–316.
7. **Chun, S. Y., and J. S. Parkinson.** 1988. Bacterial motility: membrane topology of the *Escherichia coli* MotB protein. Science **239:**276–278.
8. **Dean, G. E., R. M. Macnab, J. Stader, P. Matsumura, and C. Burks.** 1984. Gene sequence and predicted amino acid sequence of the *motA* protein, a membrane-associated protein required for flagellar rotation in *Escherichia coli*. J. Bacteriol. **159:**991–999.
9. **De Mot, R., and J. Vanderleyden.** 1994. The C-terminal sequence conservation between OmpA-related outer membrane proteins and MotB suggests a common function in both Gram-positive and Gram-negative bacteria, possibly in the interaction of these domains with peptidoglycan. Mol. Microbiol. **12:**333–334.
10. **Devereux, J., P. Haeberli, and O. Smithies.** 1984. A comprehensive set of sequence analysis programs for the VAX. Nucleic Acids Res. **12:**387–395.
11. **Dietmaier, W., S. Fabry, and R. Schmitt.** 1993. DISEC-TRISEC: di- and trinucleotide-sticky-end cloning of PCR-amplified DNA. Nucleic Acids Res. **21:**3603–3604.
12. **Fields, S., and O. Song.** 1989. A novel genetic system to detect protein-protein interactions. Nature **340:**240–241.
13. **Francis, N. R., G. E. Sosinsky, D. Thomas, and D. J. DeRosier.** 1994. Isolation, characterisation and structure of bacterial flagellar motors containing the switch complex. J. Mol. Biol. **235:**1261–1270.
14. **Götz, R., N. Limmer, K. Ober, and R. Schmitt.** 1982. Motility and chemotaxis in two strains of *Rhizobium* with complex flagella. J. Gen. Microbiol. **128:**789–798.
15. **Götz, R., and R. Schmitt.** 1987. *Rhizobium meliloti* swims by unidirectional, intermittent rotation of right-handed flagellar helices. J. Bacteriol. **169:**3146–3150.
16. **Greck, M., J. Platzer, V. Sourjik, and R. Schmitt.** 1995. Analysis of a chemotaxis operon in *Rhizobium meliloti*. Mol. Microbiol. **15:**989–1000.
17. **Haslbeck, M., W. Sterr, and R. Schmitt.** Unpublished data.
18. **Helmann, J. D.** 1991. Alternative sigma factors and the regulation of flagellar gene expression. Mol. Microbiol. **5:**2875–2882.
19. **Higuchi, R.** 1989. Using PCR to engineer DNA, p. 61–70. *In* H. A. Erlich

(ed.), PCR technology. Principles and applications for DNA amplification. Stockton Press, New York, N.Y.
20. **Hirota, N., and Y. Imae.** 1983. Na^+-driven flagellar motors of an alkalophilic *Bacillus* strain YN-1. J. Mol. Biol. Chem. **258:**10557–10581.
21. **Irikura, V. M., M. Kihara, S. Yamaguchi, H. Sockett, and R. M. Macnab.** 1993. *Salmonella typhimurium fliG* and *fliN* mutations causing defects in assembly, rotation, and switching of the flagellar motor. J. Bacteriol. **175:** 802–810.
22. **Jones, C. J., and S. Aizawa.** 1991. The bacterial flagellum and flagellar motor: structure, assembly and function. Adv. Microb. Physiol. **32:**109–172.
23. **Kamberger, W.** 1979. An Ouchterlony double diffusion study on the interaction between legume lectins and rhizobial cell surface antigens. Arch. Microbiol. **121:**83–90.
24. **Khan, S., M. Dapice, and T. H. Reese.** 1988. Effects of *mot* gene expression on the structure of the flagellar motor. J. Mol. Biol. **202:**575–584.
25. **Kihara, M., M. Homma, K. Kutsukake, and R. M. Macnab.** 1989. Flagellar switch of *Salmonella typhimurium*: gene sequences and deduced protein sequences. J. Bacteriol. **171:**3247–3257.
26. **Koebnik, R.** 1995. Proposal for a peptidoglycan-associating alpha-helical motif in the C-terminal regions of some bacterial cell-surface proteins. Mol. Microbiol. **16:**1269–1270.
27. **Krupski, G., R. Götz, K. Ober, E. Pleier, and R. Schmitt.** 1985. Structure of complex flagellar filaments in *Rhizobium meliloti*. J. Bacteriol. **162:**361–366.
28. **Kyte, J., and R. F. Doolittle.** 1982. A simple method for displaying the hydropathic character of a protein. J. Mol. Biol. **157:**105–132.
29. **Labes, M., A. Pühler, and R. Simon.** 1990. A new family of RSF1010-derived expression and *lac*-fusion broad-host-range vectors for gram-negative bacteria. Gene **89:**37–46.
30. **Larsen, S. H., R. W. Reader, E. N. Kort, W.-W. Tso, and J. Adler.** 1974. Change in direction of flagellar rotation is the basis of the chemotactic response in *Escherichia coli*. Nature **249:**74–77.
31. **Lehrer, R. J., A. Barton, and T. Ganz.** 1988. Concurrent assessment of inner and outer membrane permeabilization and bacteriolysis in *E. coli* by multiple-wave length spectrophotometry. J. Immunol. Methods **108:**153–158.
32. **Li, M., and H. P. Schweizer.** 1993. Resolution of common DNA sequencing ambiguities of GC-rich DNA templates by terminal deoxynucleotidyl transferase without dGTP analogues. Focus **14/15:**19–20.
33. **Long, S., S. McCune, and G. C. Walker.** 1988. Symbiotic loci of *Rhizobium meliloti* identified by random Tn*phoA* mutagenesis. J. Bacteriol. **170:**4257–4265.
34. **Luria, S. E., F. N. Adams, and R. C. Ting.** 1960. Transduction of lactose utilizing ability among strains of *E. coli* and *S. dysenteriae* and the properties of the transducing phage particles. Virology **12:**348–390.
35. **Macnab, R. M.** 1996. Flagella and motility, p. 123–145. *In* F. C. Neidhardt, R. Curtiss III, J. L. Ingraham, E. C. C. Lin, K. B. Low, B. Magasanik, W. S. Reznikoff, M. Riley, M. Schaechter, and H. E. Umbarger (ed.), *Escherichia coli* and *Salmonella*: cellular and molecular biology, 2nd ed. American Society for Microbiology, Washington, D.C.
36. **Malakooti, J., Y. Komeda, and P. Matsumara.** 1989. DNA sequence analysis, gene product identification, and localization of flagellar motor components of *Escherichia coli*. J. Bacteriol. **171:**2728–2734.
37. **Manson, M. D., P. Tedesco, H. C. Berg, F. M. Harold, and C. van der Driftc.** 1977. A proton motive force drives bacterial flagella. Proc. Natl. Acad. Sci. USA **74:**3060–3064.
38. **Marsh, J. L., M. Erfle, and E. J. Wykes.** 1984. The plC plasmid and phage vectors with versatile cloning sites for recombinant selection by insertional inactivation. Gene **32:**482–485.
39. **Martin, J. L., G. Waksman, J. C. A. Bardwell, J. Beckwith, and J. Kuriyan.** 1993. Crystallization of DsbA, an *E. coli* protein required for disulphide band formation *in vivo*. J. Mol. Biol. **230:**1097–1100.
40. **Maruyama, M., G. Lodderstaedt, and R. Schmitt.** 1978. Purification and biochemical properties of complex flagella isolated from *Rhizobium lupini* H13-3. Biochim. Biophys. Acta **535:**110–124.
41. **Matsuura, S., J. Shioi, and Y. Imae.** 1977. Motility in *Bacillus subtilis* driven by an artificial proton motive force. FEBS Lett. **82:**187–190.
42. **Miller, J. H.** 1972. Experiments in molecular genetics. Cold Spring Harbor Laboratory Press, Cold Spring Harbor, N.Y.
43. **Mirel, D. B., V. M. Lustre, and M. J. Chamberlin.** 1992. An operon of *Bacillus subtilis* motility genes transcribed by the sigma-D form of RNA polymerase. J. Bacteriol. **174:**4197–4204.
44. **Novick, R. P., R. C. Clowes, S. N. Cohen, R. Curtis, N. Datta, and S. Falkow.** 1976. Uniform nomenclature for bacterial plasmids: a proposal. Bacteriol. Rev. **40:**168–189.
45. **Olsen, G. J., C. R. Woese, and R. Overbeek.** 1994. The winds of (evolutionary) change: breathing new life into microbiology. J. Bacteriol. **176:**1–6.
46. **Oppenheim, D. S., and C. Yanofsky.** 1980. Translational coupling during expression of the tryptophan operon of *Escherichia coli*. Genetics **95:**785–795.
47. **Pleier, E., and R. Schmitt.** 1989. Identification and sequence analysis of two related flagellin genes in *Rhizobium meliloti*. J. Bacteriol. **173:**1467–1476.
48. **Pleier, E., and R. Schmitt.** 1991. Expression of two *Rhizobium meliloti* genes and their contribution to the complex filament structure. J. Bacteriol. **173:** 2077–2085.
49. **Pugsley, A. P.** 1993. The complete general secretory pathway in gram-negative bacteria. Microbiol. Rev. **57:**50–108.
50. **Rosenberg, A. H., B. N. Lade, D. Chui, S. Lin, J. J. Dunn, and F. W. Studier.** 1987. Vectors for selective expression of cloned DNAs by T7 RNA polymerase. Gene **56:**125–135.
51. **Sambrook, J., E. F. Fritsch, and T. Maniatis.** 1989. Molecular cloning: a laboratory manual, 2nd ed. Cold Spring Harbor Laboratory Press, Cold Spring Harbor, N.Y.
52. **Sanger, F., S. Nicklen, and A. R. Coulson.** 1977. DNA sequencing with chain-terminating inhibitors. Proc. Natl. Acad. Sci. USA **74:**5463–5467.
53. **Schäfer, A., A. Tauch, W. Jäger, J. Kalinowski, G. Thierbach, and A. Pühler.** 1994. Small mobilizable multi-purpose cloning vectors derived from the *Escherichia coli* plasmids pK18 and pK19: selection of defined deletions in the chromosome of *Corynebacterium glutamicum*. Gene **145:**69–73.
54. **Schuster, S. C., and S. Khan.** 1994. The bacterial flagellar motor. Annu. Rev. Biophys. Biomol. Struct. **23:**509–539.
55. **Selbitschka, W., S. Niemann, and A. Pühler.** 1993. Construction of gene replacement vectors for $Gram^-$ bacteria using a genetically modified *sac*RB gene as positive selection marker. Appl. Microbiol. Biotechnol. **38:**615–618.
56. **Shao, Z., J. Platzer, and R. Schmitt.** Unpublished data.
57. **Shine, J., and L. Dalgarno.** 1974. The 3′ terminal sequence of *Escherichia coli* 16S ribosomal RNA: complementary to nonsense triplets and ribosome binding sites. Proc. Natl. Acad. Sci. USA **71:**1342–1346.
58. **Simon, R., M. O'Connell, M. Labes, and A. Pühler.** 1986. Plasmid vectors for the genetic analysis and manipulation of rhizobia and other Gram-negative bacteria. Methods Enzymol. **118:**640–659.
59. **Sockett, H., S. Yamaguchi, M. Kihara, V. M. Irikura, and R. M. Macnab.** 1992. Molecular analysis of the flagellar switch protein FliM of *Salmonella typhimurium*. J. Bacteriol. **174:**793–806.
60. **Sourjik, V., and R. Schmitt.** 1996. Different roles of CheY1 and CheY2 in the chemotaxis of *Rhizobium meliloti*. Mol. Microbiol. **22:**427–436.
61. **Stader, J., P. Matsumura, D. Vacante, G. E. Dean, and R. M. Macnab.** 1986. Nucleotide sequence of the *Escherichia coli motB* gene and site-limited incorporation of its product into the cytoplasmic membrane. J. Bacteriol. **166:**244–252.
62. **Sterr, W.** 1995. Diploma thesis. University of Regensburg, Regensburg, Germany.
63. **Stolz, B., and H. C. Berg.** 1991. Evidence for interactions between MotA and MotB, torque-generating elements of the flagellar motor of *Escherichia coli*. J. Bacteriol. **173:**7033–7037.
64. **Studier, F. W., and B. A. Moffat.** 1986. Use of bacterial T7 RNA polymerase to direct selective high-level expression of cloned genes. J. Mol. Biol. **189:** 113–130.
65. **Togashi, F., S. Yamaguchi, M. Kihara, S.-I. Aizawa, and R. M. Macnab.** 1997. An extreme clockwise switch bias mutation in *fliG* of *Salmonella typhimurium* and its suppression by slow-motile mutations in *motA* and *motB*. J. Bacteriol. **179:**2994–3003.
66. **Trachtenberg, S., D. J. De Rosier, S.-I. Aizawa, and R. M. Macnab.** 1987. Three-dimensional structure of the complex flagellar filament of *Rhizobium lupini* and its relation to the structure of the plain filament. J. Mol. Biol. **195:**603–620.
67. **Wilson, M. L., and R. M. Macnab.** 1990. Co-overproduction and localization of the *Escherichia coli* motility proteins MotA and MotB. J. Bacteriol. **172:** 3932–3939.
68. **Yanisch-Perron, C., J. Vieira, and J. Messing.** 1985. Improved M13 phage cloning vectors and host strains: nucleotide sequences of the M13mp18 and pUC19 vectors. Gene **33:**103–119.